In Press, Combustion and Flame, July

Measurements of DME/Air Mixture Burning Velocities by Using Particle Image Velocimetry

Z. Zhao, A. Kazakov, and F.L. Dryer

Department of Mechanical and Aerospace Engineering
Princeton University
Princeton, New Jersey
Princeton, NJ 08544

Type of article: Full length

Corresponding author:
Frederick L. Dryer
Department of Mechanical and Aerospace Engineering
Princeton University
Princeton, New Jersey 08544
Phone: (609) 259-0316
Fax: (609) 258-1939
Email: fldryer@princeton.edu

Abstract

The laminar flame speed of Dimethyl Ether (DME)/air mixtures at room temperature and atmospheric pressure were determined experimentally over an extensive range of equivalence ratios, with and without 15% nitrogen dilution, using Particle Image Velocimetry (PIV) and a stagnation flame burner configuration. The laminar flame speeds were determined by linear extrapolation of the measured reference flame speed versus stretch rate to zero stretch rate. Experimental results are compared with available literature data and predictions of the model based on the recently published detailed reaction mechanism of DME oxidation [8,9]. The measurements are significantly higher at all equivalence ratios than the data recently reported from spherical bomb experiments. A comparison of laminar flame speed calculations using a DME oxidation mechanism developed earlier in our laboratory agrees reasonably well with the present experimental data, without modifications. Differences from prior calculations using this mechanism reported by Daly et al. [18] are resolved to be as a result of differences in numerical constraints rather than kinetics or transport databases. Modifications of the mechanism suggested in [18] are not compatible with DME validation results in the original mechanism development or with flame speed predictions for other simple fuels such as methane.

Keywords: laminar flame speed, DME, PIV, dilution, mechanism

Introduction

Both to supplement transportation fuels with non-petroleum based materials and to improve emissions of internal combustion engines, alternative fuel candidates such as Dimethyl Ether (DME) continue to receive considerable attention. DME is an attractive alternative fuel for compression-ignition (Diesel) engines because it has no carbon-carbon bonds (low sooting potential), a high cetane number of 55-60, a low boiling point of -25^{o}C, high oxygen content of 35% by weight and excellent auto-ignition characteristics [1]. Although it is a gas at room conditions, DME can be easily liquefied under pressure because of its low saturation vapor

pressure (6.1 atm at 25°C). DME is environmentally benign, virtually non-toxic, easily degraded in the troposphere and thus not harmful to the ozone layer. DME can be produced from coal and/or biomass, in addition or as an alternative to methanol, by the dehydration of methanol, or directly from natural gas in large quantities at low cost [2]. As a result of its physical combustion properties, DME is also under consideration as an alternative to liquefied petroleum gases in wider applications not involving reciprocating piston engines [3].

For piston engine applications, DME has been shown to have superior performance in conventional diesels as a neat fuel, fuel additive or an ignition enhancer [1, 4, 5]. The advantages of using DME are the very low emissions of nitrogen oxides (NO_x), reduction of the engine noise, elimination of the particulate emissions and high diesel thermal efficiency [1,4]. However, additional design optimization for operation of compression ignition engines in homogenous charge conditions on DME (and other fuels) has the potential to further improve upon these favorable results. Recent interest in homogeneous charge compression ignition (HCCI) with DME as the fuel has resulted in the use of both reduced and detailed mechanisms for DME oxidation in numerical simulations to evaluate the kinetic aspects controlling autoignition and heat release under HCCI operation [6,7]. In fact, the use of DME in HCCI modes of operation appears to yield some interesting potential for adjusting ignition characteristics in comparison to heat release rate by addition of methanol or formaldehyde. The validity of the kinetic aspects of such studies depends not only on the comparison of calculated results with experimental measurements in engines themselves, but upon the original development of the detailed kinetic mechanism utilized and its validation against fundamental chemical kinetic observations in less complex conditions than those found in diesel operation.

In the case of DME, a detailed kinetic mechanism of DME oxidation was recently developed in our laboratory in collaboration with Curran, based upon studies in a variable-pressure flow reactor over a temperature range of 550-850K at the pressures of 12-18 atm. [8,9]. We also

showed that the model reproduced the low temperature results from a jet-stirred reactor [10] and the shock-tube data [11] utilized in earlier DME mechanism studies by Curran et al. [12] and Dagaut et al. [10]. At the time of publication, however, few data were available from laminar flame studies with which computations using the mechanism could be compared.

Several such studies have appeared since. Kaiser et al. [13] used the model appearing in [9] to compare computed results with species profiles measured in an atmospheric pressure, burner-stabilized DME/air laminar premixed flame. Sources for the transport data are specified in the paper, but the specific data used from the various sources is not identified. The sources of some differences in the computational results depending on whether the computations were made using CHEMKIN [14]/PREMIX [15] or HCT [16] codes could not be specifically determined, but Kaiser et al. report reasonable agreement between the model predictions and the experimental data. The computed peak mole fractions of reactant, intermediate, and product species agreed to within 30% with the experimental peak mole fractions for all flames except the lean case. For lean conditions, the predicted flame thickness was much narrower and the predicted intermediate hydrocarbon species mole fractions, with the exception of CH_2O, were over-predicted by about a factor of three. The authors note, however, that the computational/experimental comparison supports that the kinetic mechanism is essentially correct, with the decomposition of the methoxymethyl radical as the major source of formaldehyde and methyl radicals (which can lead to C_2 species and sooting under very fuel rich conditions). It was further speculated that the discrepancies of lean conditions might originate from the absence of reactions involving activated species, e.g.,

$$CH_2O + OH \rightarrow HOCH_2O^* \rightarrow HOCHO + H$$

In another study, McIlroy et al. [17] compared predictions using the mechanism of [9] and transport coefficients developed in [13] to predict low pressure burner stabilized laminar flame species profiles for DME/oxygen/Argon flames at 30 torr and 0.98 and 1.2 equivalence ratios.

Using the flame temperature profiles as input, species profiles for DME, O_2, CO, CO_2, H_2O, H_2, CH_2O, CH_4, HCCH, and two radicals, OH and CH_3, were compared with computations as a function of height above the burner surface. Generally, good agreement was found between the model and data for stable species, with the largest discrepancies occurring for methyl radical profiles. The model appeared to predict qualitatively different trends in the methyl radical concentration with stoichiometry than observed in the experiment; methyl radicals increased with increasing stoichiometry in the predictions, while the experiment showed a decrease.

The above two flame studies suggest reasonable behavior of this DME mechanism at flame conditions. However, Daly et al. [18] recently published laminar flame speed experimental data using spherical bomb techniques that suggest that the performance of the mechanism published in [9] is inferior in predicting DME laminar flame speeds. Predictions based on both this mechanism and an earlier one [12] using the transport coefficients developed in [13] differ substantially from their reported experimental measurements. Daly et al. made spherical bomb measurements with both compressed air, and a synthetic mixture composed of 80% nitrogen and 20% oxygen. Daly et al. claimed that the predictions using the mechanism from [12] produce laminar flame speeds lower than the reported experimental measurements, particularly for fuel lean conditions, while those utilizing the mechanism of [9] were uniformly considerably higher than the experiment over the entire range of equivalence ratios studied. Daly et al. discarded further study of mechanism in [12] and attempted to remove the disparity with the predictions using the mechanism of [9] by changing the following reaction rate constants by a factor of ½, 12, and 3, respectively:

$$HCO + M = CO + H + M \quad (12)$$

$$HCO + H = CO + H_2 \quad (6)$$

$$HCO + CH_3 = CH_4 + CO \quad (39)$$

While the modifications resulted in better agreement of predictions with fuel lean experimental results, agreement with fuel rich results deteriorated. The effects of adjustments of these rate constants on any of the comparisons with the original data used in developing the mechanism or with published values, or flame speed predictions for other simple fuels such as methane or formaldehyde were not investigated.

Laminar flame speed is an important property of the combustible mixture because it embodies fundamental information on diffusivity, reactivity, and heat release rate of the mixture. In turbulent combustion modeling and the engine design, knowledge of laminar flame speed is very beneficial to predicting burning rate. Because of the significance of laminar flame speed information, substantial experimental work has been devoted over the years to develop methodologies for accurate determination of laminar flame speeds. The major experimental difficulties are the achievement of a planar, stationary and adiabatic flame, and the determination of flame front. Although there is no general consensus on the best approach used to measure laminar flame speed, spherical bomb methods and stagnation flames are presently considered to be the most systematic and accurate approaches.

In the conventional spherical-bomb method utilized by Daly et al., the combustible mixture is produced inside a spherical vessel, and upon ignition at its center, a spherical flame propagates outward, producing a continuous change of the temperature and pressure of the unburned mixture. The flame speed can be determined by measuring the rate of change of pressure using transducers or the rate of change of flame radius by diagnostic methods such as Schlieren imaging. Potential experimental sources of inaccuracy are non-spherical flame distortion produced by ignition and buoyancy, heat loss to the electrodes generally used for ignition, flame stretch effects, and development of intrinsic pulsating and cellular instabilities over the flame surface. More importantly, analyses of the raw data to yield flame speed relies on a number of assumptions on the burned and unburned gases and adiabatic conditions in the burned gases to estimate the

movement of unburned gases relative to the laboratory reference frame. As a result, the laminar flame speed is determined as a small difference between two relatively large numbers (flame and unburned gas velocities relative to the laboratory reference frame), and is subject to a significant experimental uncertainty [19]. The advantage of spherical bomb methods over stagnation flame methods is primarily in the fact that the effects of ambient pressure on flame speed can be investigated over the wider range of pressure conditions more easily than in the stagnation methods discussed below.

Principal advantages of stagnation flame methods are that the unburned gas velocities and flame speeds are of the same order of magnitude, the experiment itself is essentially quasi-steady at constant pressure, and flow field measurements can be used to determine the required velocities, flame stretch, and flame position. Moreover, the influence of flame stretch on laminar flame speed can be experimentally assessed from data obtained with stretch as an independent variable. In the stagnation flame method, one or two planar, steady, nearly one-dimensional laminar flames are obtained by impinging a nozzle-generated uniform combustible flow onto either a flat plate, or an identical combustible flow. The flame(s) is (are) stabilized by aerodynamic strain rate in the flow field. The velocity component, υ, along the axis first decreases as the flow moves towards the stagnation plate, and then increases due to the thermal expansion as the flow enters the flame zone. After passing the flame, υ decreases again when the flow approaches the stagnation plane. The stretch rate can be determined based upon the quasi-linear velocity gradient which occurs just before the flow reaches the preheat zone. The minimum velocity can be recognized as the reference flame speed. By linear or nonlinear [20,21] extrapolation to the zero stretch point on plots of strain rates and reference flame speeds, the laminar flame speeds, s_u^o, can be obtained.

In the specific case of DME/air flames, the pioneering work of Gibbs and Calcote [22], and the data set of Daly et al. [18], both involve influences of flame stretch, for which no corrections were applied. Our experiments were initiated prior to the appearance of the work of Daly et al.,

with similar motivation (i.e., to supply additional flame speed data), but specifically to supply reference measurements for DME/ air mixtures for which the flame stretch effects had been removed. The disparities of both our experimental and computational results with those of Daly et al., as discussed in more detail below, were recognized early on [23]. The present paper presents the details of the experimental measurements, their comparison with other available data, and discusses disparities in the present calculations and those of Daly et al.

Experimental Methodology

The experimental configuration used in the present work is a modification of the single jet-wall stagnation flame, first introduced by Egolfopoulos et al. [24], and is briefly described below. The present experiments were performed early in our adaptation of using Particle Image Velocimetry (PIV) in determining laminar flame speeds. Only recently have researchers, e.g., [25] including us [23] begun to apply this technique to laminar flame speed measurements. The advantage of PIV over Laser Doppler Anemometry (LDA) is that for each experimental condition, both the velocity and velocity gradient can be determined throughout an entire two dimensional flow field simultaneously. Both PIV and LDA employ small (< 1 μm) tracer particles added to the flow, to closely follow the fluid motion, but applications of these techniques in other venues have well characterized the issues of seeding density and particle size on particle slip, etc., and these results can be immediately applied to laminar flame environments. The remaining issues of seeding perturbations to combustion have also been addressed previously, and since the required seeding densities of PIV and LDA are similar, these issues also need no additional consideration.

In PIV, knowing the time between consecutive images of the tracer particle motions, the velocity field is obtained from the displacement of the tracers. Either a pulsed laser or a shuttered CW laser can be used as a light source, with the optical beam shaped into a thin light sheet using cylindrical lenses. Either multi-exposure single images or single-exposure multiple images can be

used according to different image interrogation methods, among which spatial correlation methods are conventional [26].

The majority of the experimental measurements reported here were obtained in an experimental burner and stagnation plate setup that was an early version of a more refined apparatus for laminar flame speed measurements discussed in [27]. This early version was designed to investigate only gaseous fuel/air flame speeds at room temperature conditions and atmospheric pressure, while that described in [27] can accommodate both liquid and gaseous fuels and vary unburned gas temperatures up to 600 K. Measurements that were made for DME/air flames diluted with nitrogen were performed in the more recent apparatus. Both experiments utilize identical burner and stagnation plate designs, and reference experiments were performed to assure the equivalence of identical measurements on the early and more recent embodiments.

The burner configuration directs a premixed, seeded reactant flow upward from a 14 mm converging nozzle situated at the center of a water-cooled burner surface. The burner flow is impinged vertically upward, orthogonally, onto an 8.9 cm diameter, silica foam flat plate. Silica foam is used as the stagnation surface because the material has a much lower conductivity and heat capacity than stainless steel. This material provides near-adiabatic conditions, but continues to result in radiative loss on gas temperatures in close contact with the plate surface. The burner flow is shrouded by a 2 mm annular flow of nitrogen to stabilize the flame. The flow field disturbances resulting from the shroud flow and burner exit to stagnation wall distance (25 mm) were shown to be negligible, experimentally. Enclosures of the burner/stagnation plate were utilized to contain the seeded burner exhaust gases and the exhausted materials were directed to a wet scrubber to filter out seeding particles, prior to purging the flow into a house exhaust system.

While fuel and airflow system configurations are somewhat different in the earlier and most recent experimental configurations, the general flow control and measurement methods are identical. Compressed cylinder air and DME gas were supplied by two stage regulators through

sonic nozzle metering valves. The metered flows were mixed and diverted through a particle seeder containing 0.3-0.7 micron Boron-Nitride particles. The particle-laden mixture exiting the seeder was then separated into two parts using two needle valves to control the relative pressure drop of the two downstream channels. One part of the mixture was diverted to the burner and the other was diverted directly to the exhaust scrubber system, thus allowing the variation of the burner flow velocity without manipulating the individual flow rates of each component (affecting uncertainty in the flow equivalence ratio). Because DME is soluble in water (one volume water can dissolve up to 37 volumes of gas), wet test meter measurements could not be used directly to determine DME flow rates. Instead, a wet test meter was used to calibrate a Hastings mass flow meter operating on nitrogen, and the DME measurements were made using the calibrated Hastings meter corrected for the differences in molecular properties. The flow rate of the air was determined using the wet test meter. In performing experiments, meter measurements were performed for DME and air at each set of measurements performed at the same equivalence ratio, but with different burner flow rates. Thus uncertainty of each equivalence ratio studied was less than $\pm$ 0.01.

In early measurements, we used a chopper shuttered Argon Ion laser as a light source, but in some of the later measurements, a Continuum® Minilite PIV Nd:Yag laser was employed. Uncertainty differences in the laser shutter timing and pulse repetition were inconsequential to determining the PIV flow field velocities in the region utilized for measurements and over the range of measured flame speeds.

The flow field images at different times were recorded using either a 35 mm film camera or a Kodak DCS 460 digital camera (3060x2036 pixels). Digital representations of the images were subsequently analyzed using an in-house code [28] with auto-correlation method.

Uncertainties in velocity measurement using any optical method that tracks particle motion also depend on the statistics gathered from multiple events as well as the optical “interrogation”

cell window within which the sampling occurs. In the case of PIV, there is a trade-off between seeding density and interrogation window size on the number of statistically significant particle displacement measurements. While increasing the size of the window improves the statistics, it may also limit the spatial resolution of the PIV determined velocity, since the average particle velocity within the window may be skewed. We have investigated this relationship to find the appropriate spatial resolution for the present application. Figures 1 presents the particle displacement determined at fixed displacement time for the same image with different interrogation window size. As window size is decreased, seeding must be increased to maintain sufficient number of particles within the window to achieve appropriate statistical sampling. Eventually, the statistics decay because of multiple particle images in the depth of field (overlapping particle images). It was found that 64 x 64 pixel interrogation was sufficiently small to yield good spatial resolution in the measurement without inordinate degradations in statistical sampling. Other details concerning the experimental methodology, experimental uncertainties, etc. appear in reference 23.

Results and Discussion

As mentioned earlier, PIV can determine the velocity map of the entire two-dimensional flow field nearly instantaneously. Figure 2 is an exemplar vector map obtained from the PIV interrogation code. The particle density and displacement between the two exposures were chosen to optimize the correlation results for auto-correlation. Beyond the position of the leading edge of flame front, thermal expansion leads to flow acceleration, and the resulting reduced particle density becomes too low to obtain reliable velocity vectors from correlation. This feature clearly defines the flame front location. Figure 3 shows the velocity profile on the centerline of the flow. The minimum point in this velocity profile was defined as the flame speed for the measured stretch rate, and the stretch rate was determined based upon the quasi-linear gradient portion of the

approaching velocity profile. Linear extrapolation of the measured flame speed as a function of measured stretch rate was used to obtain the zero stretched reference laminar flame speed. The direction of the velocity in stagnation flow is well defined, thus avoiding a directional ambiguity characteristic of auto-correlation methodology. Presence of the wall in the jet-wall setup allows stable flame position at lower strain rates than with the opposed-jet configuration. Performing measurements at lower strain rates is important to minimizing uncertainties in determining zero-stretch flame speed through extrapolation, especially when the strain rate and the reference flame speed measurements are inherently scattered [23].

Measured DME/Air flame speed

Our measured DME/Air flame speeds for different equivalence ratios and with 15% nitrogen dilution are reported in Fig. 4. Detailed error analysis of our measurements described elsewhere [27] yields an uncertainty of less than 5 %. Also shown are data in the published literature from Gibbs and Calcote [22] and from Daly et al [18]. Daly et al. report room temperature flame speed data for both DME/air and DME/synthetic-air (20%O_2 and 80%N_2) mixtures. From the Figure, it is clear that the flame speeds for these different oxygen contents nearly overlap for fuel lean conditions.

While our flame speed measurements for room temperature DME/air mixtures differ in shape with equivalence ratio changes from those of Gibbs and Calcote [22], the two sets of data partially overlap at maximum flame speed conditions. Daly et al. [18] estimate the uncertainty in their measurements by analogy with similar spherical bomb experiments reported in the literature at 5%. Based on this estimate, we can conclude there is a borderline overlap of their data and the data reported here at fuel-lean and near-stoichiometric conditions. At fuel rich conditions, the disparities between the two sets of data appear to be more pronounced. However, it should be noted that our uncertainties in measurements at fuel rich conditions are larger than those at lean/

stoichiometric conditions due to flame instability effects (the results of Daly et al. should also be affected by this problem). These issues are apparent particularly at $\varphi > 1.5$. As a result, the shape of the laminar flame speed curve at rich conditions should not be strictly inferred from the data. Finally it should be noted that the present DME/air flame speed data are consistently higher than those of Daly et al. at all but very lean equivalence ratios.

Modeling results obtained in the present study are also compared with experimental measurements in Fig. 4. We computed DME laminar flame speeds with the PREMIX [15] code of the Sandia CHEMKIN II package [14] and our recently published DME oxidation mechanism [8,9]. The majority of transport parameters we used were taken from the Sandia database [29] and the compilation of Reid et al. [30]. Transport parameters that were not available in the literature were estimated using the techniques described in Ref. 31.

We immediately noted that our computational predictions for DME/air flame speeds were substantially displaced from these of Daly et al. [18]. In personnel correspondence with the authors and exchange of results [32], we found that Daly et al. [18] used nearly the same reaction mechanism as ours [8,9] with only minor differences [13]. Our analyses showed that neither mechanistic differences or differences in transport databases could account for the disparities in the computed results. Further computational studies and subsequent communication with the authors [32], however, conclusively showed that the majority of differences were due to insufficient refinement in grid resolution (less than 100 grid points) in the PREMIX calculations of Daly et al. [18]. PREMIX calculations with different grid resolutions were performed and it was found that a resolution of 400 grid points and above yielded sufficiently converged flame speed predictions. In the present work, in order to guarantee the accuracy of the prediction, a very fine grid resolution (up to 1000 points) was tested.

In Fig. 4, we note that both DME/air and diluted DME/air laminar flame speeds that we computed with the DME mechanism published in [8,9] (without any modifications, and with the

above grid resolutions) agree reasonably well with all of the experimental DME/air flame speed data. Unlike the experimental results of Daly et al., the predicted laminar flame speed decreases significantly with decreasing oxygen concentration (21% versus 20%) over all equivalence ratios. The predicted flame speed of DME/air at $\varphi = 1.0$ is 10% higher than that of DME/synthetic-air ($20\%O_2$ and $80\%N_2$) mixtures. The experimental data of Daly et al. [18] appear to exhibit different trend; in fact, the flame speed for DME/synthetic-air mixture higher than that for DME/air mixture at $\varphi = 1.0$.

To illustrate the influence of individual reaction rates on predicted flame speeds, a sensitivity analysis was performed for three selected cases of lean, stoichiometric, and rich mixture compositions, and these results are presented in Fig. 5. The sensitivity spectrum for DME/air flames exhibits the features typically seen and well documented for flames of small hydrocarbons [33,34], and the results are qualitatively similar to those reported in Daly et al. The spectrum is dominated by the main chain branching reaction,

$H + O_2 = OH + O$,

formyl decomposition,

$HCO + M = CO + H + M$,

and CO oxidation,

$CO + OH = CO_2 + H$.

The reactions that are specific to DME contribute noticeably only for the rich case ($\phi = 1.4$), i.e., unimolecular decomposition of DME,

$CH_3OCH_3 = CH_3 + CH_3O$,

and H abstraction from DME by H atom,

$CH_3OCH_3 + H = CH_3OCH_2 + H_2$.

While it is possible to further improve the agreement between the model predictions and the present data by adjusting less established rate coefficients, the present agreement appears to be

well within the experimental uncertainty of our measurements. Computational uncertainties may also come from elsewhere, such as from the transport model [29] or radiative heat losses present in the experiments (and unaccounted for in the calculations). We have recently estimated the effects of radiative loss in other flame speed computations on propane/air mixtures, and we found the corrections to be small in comparison to other uncertainties and important only near the flammability limits [27].

Based upon the disparity of their computations and experiments, Daly et al attempted to reconcile differences by adjusting rate constants for the three key reactions of formyl radical, (12), (6), and (39) appearing in Fig. 5. We do not believe that the present level of agreement shown here is in itself sufficient motivation or constraint to modify the present mechanism as they describe. In investigating their modifications further, we found that they lead to substantial deterioration in the comparison of predictions with the DME flow reactor and other data appearing in [8,9] that were used in the original mechanism validation. Moreover, modifications in kinetics and thermo chemistry should not be performed based upon improving this agreement without investigating the result of the changes in predictions of fundamental kinetics observations used in initially validating the mechanism and against flame speed measurements for other simple fuels. In addition, these three reactions are present in sensitivity maps similar to that of Fig. 5 based upon flame speed computations for numerous other fuels, including CH_4, C_3H_8, and larger carbon number species such as n-heptane and n-decane. As a result, further improvement of DME flame speed computations with experimental data cannot be obtained through isolated analyses and modifications of only these reactions. Curran [35] has continued to evolve the DME mechanism published in [9], updating thermo chemistry and rate constant information, but at present these modifications have not been documented through predictions of available literature data.

Conclusions

Laminar flame speed for DME/Air mixtures at room temperature and atmospheric pressure without or with 15% N_2 dilution was determined on a stagnation flame using the PIV. The measured values agree well with the modeling results based on the detailed reaction mechanism of DME oxidation [8,9], but differ substantially from those DME/air data recently reported in the literature.

Acknowledgment

This work was supported by a discretionary grant from Ford Research Laboratories, NASA Glenn Research Center under NASA Grant No. NAG3-2473, and by the Chemical Sciences, Geosciences and Biosciences Division, Office of Basic Energy Sciences, Office of Science, U.S. Department of Energy under Grant No. DE-FG02-86ER13503. The authors wish to thank Dr. Steven Klotz for his early contributions to work, Dr. Boguslaw Gajdeczko and Mr. Paul Michniewicz for their technical contributions to developing the apparatus and experimental methodologies employed in the research. The DME mechanism used in this study may be obtained electronically by contacting the corresponding author.

REFERENCES

1. T.H. Fleisch, C.Mc Carthy, A. Basu, C. Udovich, P. Charbonneau, W. Slodowske, S. Mikkelsen, J. McCandless, SAE-950061.
2. B.J. Hansen, B. Voss, F. Joensen, I.D. Sigurdardottir, SAE-950063.
3. E.D. Larson, R. Tingjin, Energy for Sustainable Development, VII 4 (2003) 2-44.
4. S.C. Sorenson, S. Mikkelsen, SAE-950064.
5. M.E. Karpul, J.D. Wright, J.L. Dippo, D.E. Jantzen, SAE-912420.
6. H. Yamada, H. Sakansashi, H. Choi, A. Tezaki, SAE 2003-01-1819.
7. M. Konno, Z. Chen, K. Miki, SAE 2003-01-1826.

8. S. L. Fischer, F. L. Dryer, H. J. Curran, Int. J. Chem. Kinet., 32 (2000) 713-740.
9. H. J. Curran S. L. Fischer, F. L. Dryer, Int. J. Chem. Kinet., 32 (2000) 741-759.
10. P. Dagaut, C. Daly, J.M. Simmie, M. Cathonnet, Proc. Combust. Inst. 27 (1998) 361-369.
11. U. Pfahl, K. Fieweger, G. Adomeit, Proc. Combust. Inst. 26 (1996) 781-789.
12. H.J. Curran, W.J. Pitz, C.K. Westbrook, P. Dagaut, J-C. Boettner, M. Cathonnet, Int. J. Chem. Kinet., 30 (1998) 229-241.
13. E.W. Kaiser, T.J. Wallington, M.D. Hurley, J. Platz, H.J. Curran, W.J. Pitz, C.K. Westbrook, J. Phys. Chem. A 104 (2000) 8194-8206.
14. R.J. Kee, F.M. Rupley, J.A. Miller, CHEMKIN II: A Fortran Chemical Kinetics Package for the Analysis of Gas Phase Chemical Kinetics, Report No. SAND89-8009, Sandia National Laboratories, 1989.
15. R.J. Kee, J.F. Grgar, M. D. Smooke, J.A. Miller, A Fortran Program for Modeling Steady Laminar One-dimensional Premixed Flames, Report No. SAND85-8240, Sandia National Laboratories, 1985.
16. C.M. Lund, L. Chase, HCT-A General Computer Program for Calculating Time-Dependence Phenomena Involving One-Dimensional Hydrodynamics, Transport, and Detailed Chemical Kinetics, Report No. UCRL-52504, Revised, Lawrence Livermore National Laboratory 1995.
17. A. McIlroy, T.D. Hain, H.A. Michelsen, T.A. Cool, Proc Comb. Inst. 28 (2000) 1647-1653.
18. C.A. Daly, J.M. Simmie, J. Wurmel, N. DjebaIli, C. Paillard, Combust. Flame 125 (2001) 1329-1340.
19. I. Glassman, Combustion, 3rd ed., Academic Press, San Diego, 1996.
20. B.H. Chao, FN. Egolfopoulos, C.K. Law, Combust. Flame 109 (1997) 620-638.

21. C.M. Vagelopoulos, F.N. Egolfopoulos, C.K. Law, Proc. Combust. Inst. 25 (1994) 1341-1347.
22. G.J. Gibbs, H.F. Calcote, J. Chem. Eng. Data. 3 (1959) 226-235.
23. Z. Zhao, A. Kazakov, F.L. Dryer, Laminar Flame Speed Study of DME/Air MixturesUsing Particle Image Velocimetry, The 2001 Technical Meeting of the Eastern States Section of the Combustion Institute, Hilton Head, SC, 2001
24. F.N. Egolfopoulos, H. Zhang, Z. Zhang, Combust. Flame, 109 (1997) 237-252.
25. T. Hirasawa, C.J. Sung, Z. Yang, H. Wang, C.K. Law, Determination of Laminar Flame Speeds of Ethylene/n-Butane/Air Flames Using Digital Particle Image Velocimetry, 2nd Joint Meeting of the U.S. Section of the Combustion Institute, Oakland, CA, 2001.
26. I. Grant, Proc Inst. Mech. Engrs. 211 C (1997) 55-76.
27. Z. Zhao, A. Kazakov, J. Li, F.L. Dryer, The Initial Temperature and N_2 Dilution Effect on the Laminar Flame Speed of Propane/Air Mixtures, Special Issue for the 19th ICODERS Meeting, Hakone, Japan, June 25-Aug. 1, 2003 (F.A. Williams and W.A. Sirignano Eds.), Combust. Sci Tech. Accepted, January, 2004.
28. M. Stucky, E. Nino, B. Gajdeczko, P. Felton, Experimental Thermal and Fluid Science Journal 8 (1994) 305-311.
29. R.J. Kee, G. Dixon-Lewis, J. Warnatz, M.E. Coltrin, J.A. Miller, A Fortran Computer Code Package for the Evaluation of Gas-Phase, Multicomponent Transport Properties, Report No. SAND86-8246, Sandia National Laboratories, 1986.
30. R.C. Reid, J.M. Prausnitz, B.E. Poling. The Properties of Gases and Liquids, McGcraw-Hill, Inc. New York, NY, 1987.
31. H. Wang, M. Frenklach, Combust. Flame 96 (1994) 163-170.
32. J. M. Simmie, personal communication, August 2001.

33. G.P. Smith, D.M. Golden, M. Frenklach, M. Frenklach, N.W. Moriarty, B. Eiteneer, M. Goldenberg, C.T. Bowman, R.K. Hanson, S. Song, W.C. Gardiner, Jr., V.V. Lissianski, Z. Qin, http://www.me.berkeley.edu/gri_mech/.
34. Z. Qin, V. Lissianski, H. Yang, W.C. Gardiner, Jr., S.G. Davis, H. Wang, Proc. Combust. Inst. 28 (2000) 1663-1669.
35. H.J. Curran, personal communication, 2004.

List of Captions for the Figures:

Fig. 1. Effect of correlation window size on the displacement determination in PIV.

Fig. 2. Example of velocity vector map of auto-correlation PIV.

Fig. 3. Axial flow velocity versus distance from the burner for stagnation flame configuration.

Fig. 4. Measured and predicted laminar flame speed of DME/N_2/O_2 mixtures at 298 K , atmospheric pressure (lines: model prediction, symbols: experimental data).

Fig. 5. Sensitivities of kinetic parameters for laminar flame speeds of DME/air flame at various equivalence ratios.

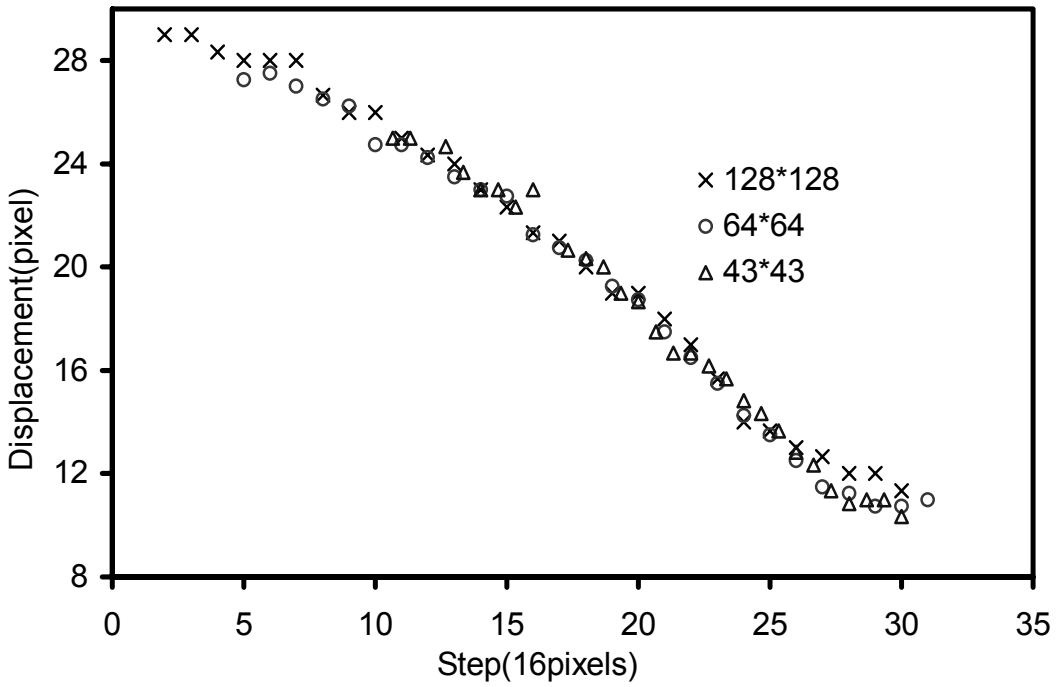

Fig. 1

Z. Zhao, A. Kazakov, and F.L. Dryer

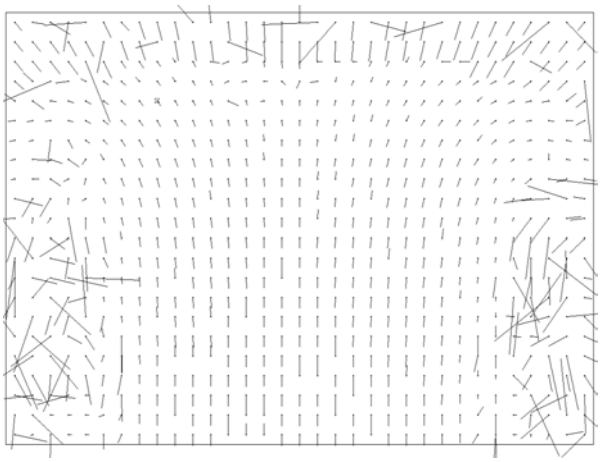

Fig. 2

Z. Zhao, A. Kazakov, and F.L. Dryer

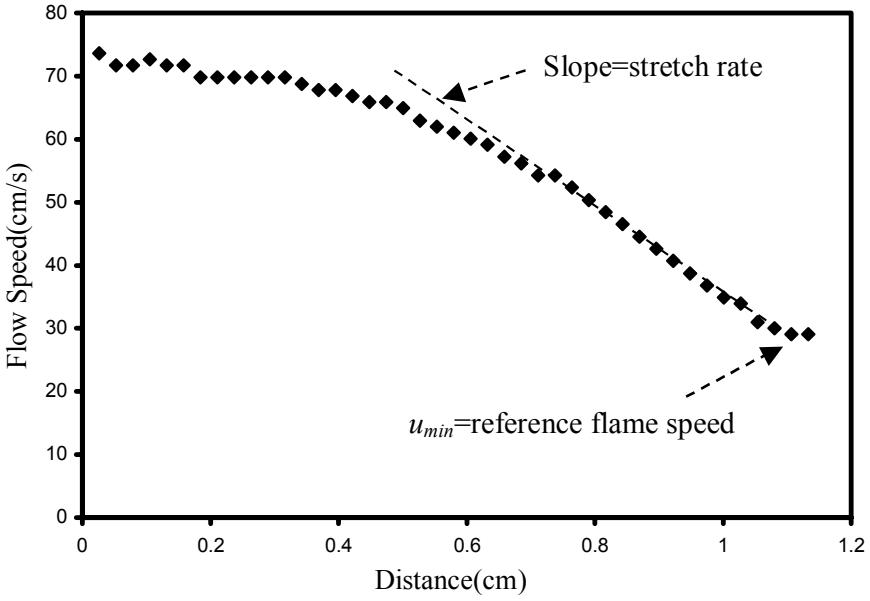

Fig. 3

Z. Zhao, A. Kazakov, and F.L. Dryer

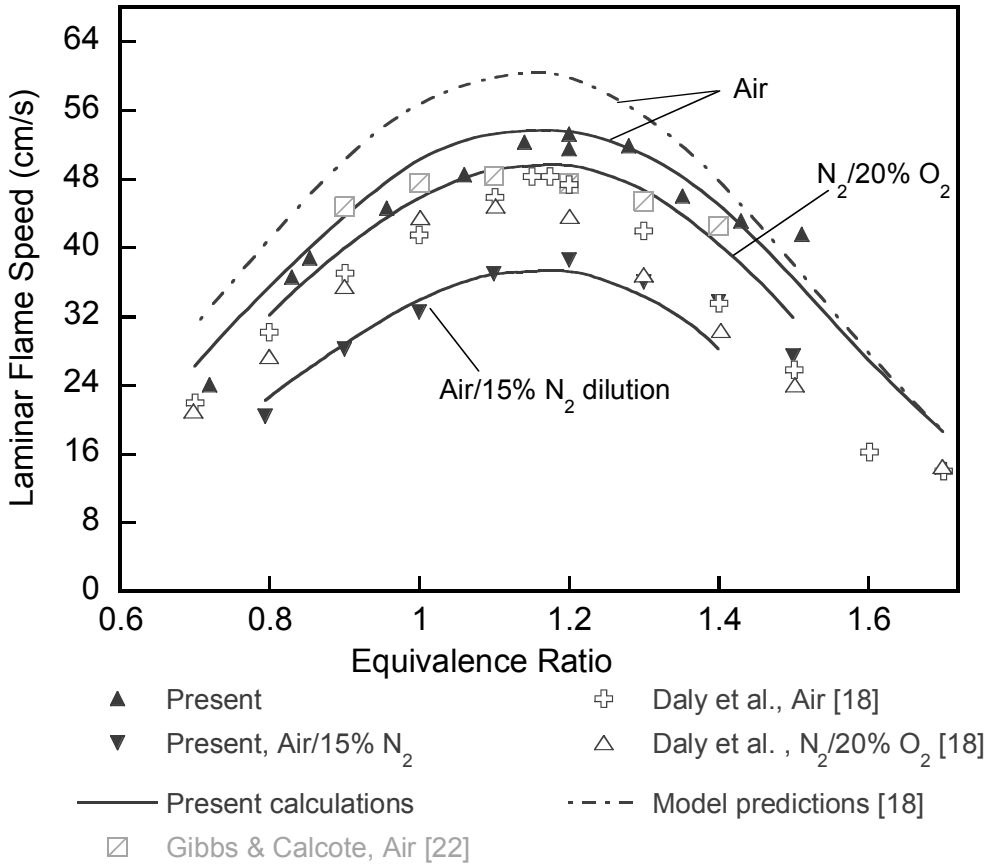

Fig. 4

Z. Zhao, A. Kazakov, and F.L. Dryer

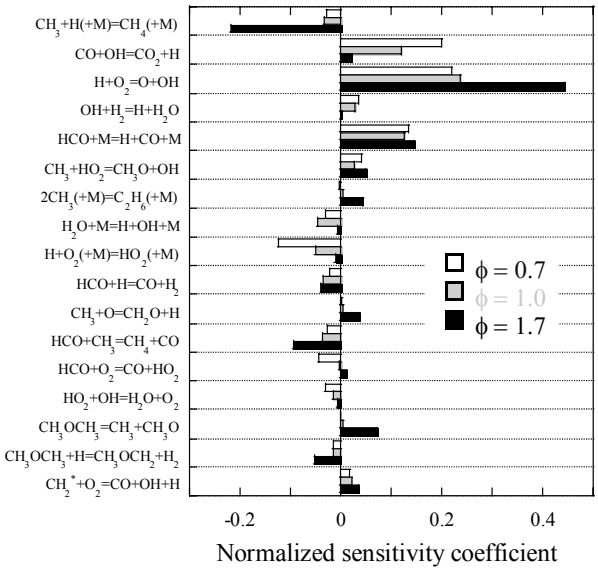

Fig. 5

Z. Zhao, A. Kazakov, and F.L. Dryer